STUDIES ON SURFACE CONDENSATION FOR PASSIVE SAFETY SYSTEM IN LIGHT WATER REACTOR A Review

by

SUSYADI [1,2]***, Mulya JUARSA*** [2]***, Nandy PUTRA*** [1]***, and Raldi A. KOESTOER*** [1*]

[1]Heat Transfer Laboratory, Department of Mechanical Engineering,
Faculty of Engineering, Universitas Indonesia, Depok, Indonesia
[2] Research Center for Nuclear Reactor Technology, National Research and Innovation Agency,
Tangerang, Selatan, Indonesia

Review paper
https://doi.org/10.2298/NTRP2304215S

A system with a passive mechanism has been considered to have better trustworthiness because it does not require an external driving force to function. Several nuclear reactor designs have implemented this feature either fully or partially in their safety systems. Some of them combine boiling and condensation phenomena to deal with decay heat when an accident occurs. This paper reviews studies on condensation heat transfer in passive residual heat removal systems and passive containment cooling systems of light water-cooled reactors. The emphasis is on the applicability of acknowledged correlations for accident conditions and its development for a better model. In the explanation, the passive mechanism and type of condenser implemented in the system are first identified. Afterward, comparative formula assessment using test data, parametric studies using computer simulation, and new correlation development are discussed. The evaluation showed that the use of existing correlation needs tuning in the case of light water reactor passive safety system design. Besides, it was also suggested to take into account the geometric form of the condensation surface. Further research on helical shape is needed to assess the possibility of an integral reactor's steam generator changing role as a condenser during the loss of coolant accident that is followed by safety system failure.

Key words: condensation, safety system, heat removal, light water reactor, accident

INTRODUCTION

The passive safety system is considered safer and more reliable in dealing with an accident than active equipment as it does not require external forces to work [1]. The use of passive features in nuclear power plants (NPP) has been known for years but gained more attention after the Fukushima accident in 2011. At that time, the natural catastrophe prevented the restoration of electric power for several days, leading to an extended station blackout (SBO) [2]. The lessons gained from the accident recommended a cooling which capable of functioning for a long time [3]. At present, some of the light water reactor (LWR) designs, including the integral typed reactors, have implemented this feature either fully or partially. Such reactors among others are the SMART, CAREM, NuScale, and IRIS for the integral type [4] and Hualong-1, APR+, and AP1000 for the large reactors [5-7].

Diverse passive cooling approaches exist in LWR. One of them is the two-phase natural circulation that is present in the passive residual heat removal system (PRHRS) [8] and the passive containment cooling system (PCCS) [9]. These systems mostly involve saturated condensation on one side and atmospheric boiling on the other.

Efforts to implement this feature have been performed using theoretical, computer modeling, and experimental approaches. However, studies on thermal performance especially for the one which involves a combination of condensation and boiling, still left various issues due to the complexity of the phenomena.

Several works related to reactor accident conditions have been conducted. de la Rosa *et al.* [10] perform a review that focuses on the condensation process on containment structure. The paper evaluates and discusses specific physical phenomena, various available models, and validation data. Overall, 20 phenomena and parameters are analyzed to capture all relevant aspects. In addition, models to predict wall condensation in the presence of non-condensable (NC)

* Corresponding author, e-mail: koestoer@eng.ui.ac.id

gas in some thermohydraulic codes are also summarized. In line with that, Yadav *et al*. [11] perform a critical review of studies on steam condensation inside containment about hydrogen combustion issues. The discussion contains an elaboration of condensation fundamentals, modeling methods, variables affecting condensation, and experiments in both integral facilities and separate effect test apparatus. In the end, it is suggested that future studies should focus on the coupled nature of the problem in an all-inclusive manner to ensure the safety of the reactor.

For a more general discussion, Huang *et al*. [12] review models, mechanisms, and experimental results for film-wise vapor condensation in the presence of NC gas. Theoretical and semi-theoretical approaches are elaborated to get insight into the process. Huang *et al*., [12] concludes that the thickness of condensate, surface waves, suction effect, and interfacial shear strength have a significant influence on the heat transfer when NC gas exists.

Although the aforementioned studies have covered many important issues in reactor accident conditions, most of the reviews do not enlighten the accuracy of the model compared with experimental data. An appropriate heat transfer correlation (HTC) for high pressure and temperature, gas presence, and two-phase flow, is necessary for NPP design to ensure safety. This paper explores studies on steam condensation in LWR's safety system, concentrating on the applicability of existing practical correlations and their development for a better model. Comparative formula assessment using test data and numerical analysis using widely used computer codes is also presented. In doing so, the passive design involving condensation in several advanced reactors is elaborated in the beginning.

REACTOR ACCIDENTS AND SAFETY SYSTEMS

The reactor safety system is designed to serve the following vital functions: control of fission reaction, removal of heat from the reactor and the spent fuel storage, and confinement of radioactive material, shielding against radiation, and control of radioactive releases [13].

When an unintended transient occurs, the protection system halts the fission by inserting control rods. A cooling system then performs tasks to achieve a safe shutdown. If leakage occurs, steam-bearing radioactive substances will be kept within the containment. Hence, structural integrity should be kept intact by controlling the pressure and temperature. Those safety necessities can be implemented to some extent with a passive system.

Passive residual heat removal system

In the loss of normal heat-sink and SBO events, the PRHRS plays a vital role in decay heat cooling. The passive mechanism taking place can be single-phase or two-phase natural circulation depending on the coupling technique implemented [14].

In PWR, the two-phase mechanism is implemented when PRHRS is coupled with a steam generator (SG). Schematic diagrams are presented in figs. 1 and 2. Steam produced in SG is directed to a condenser immersed in the open water tank. The resulting condensate is then recirculated by gravity back to the SG. The service period of this PRHRS will depend on the amount of water in the tank, which is typically 72 hours. However, its capability can be extended by adding an extra cooling system or by other means [14, 15].

In the boiling water reactor (BWR) arrangement, a system called an isolation condenser system (ICS) also uses a two-phase mechanism. Figure 2 displays a schematic diagram of the ICS. The condenser is coupled with the primary system where it condenses the steam produced by core decay heat when the system is being isolated.

An integral PWR, namely CAREM, also adopts a similar like to BWR's approach in its decay heat removal system called the Emergency Condenser System [17]. Table 1 summarizes the coupling method and type of condenser used for various reactor designs.

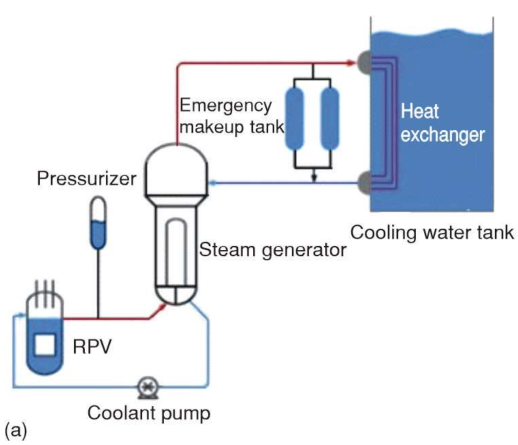

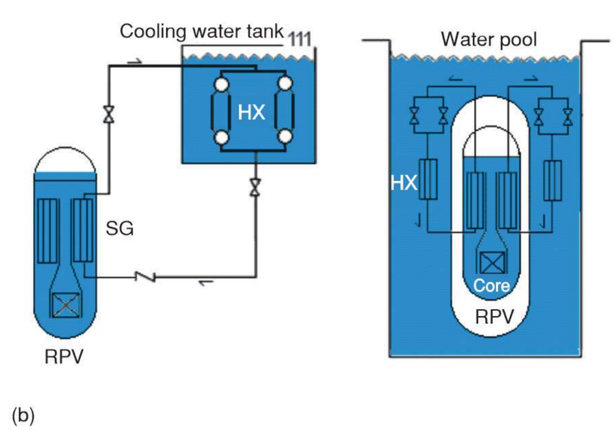

Figure 1. The PRHRS coupled with SG in conventional PWR [18] and in integral PWR [4]

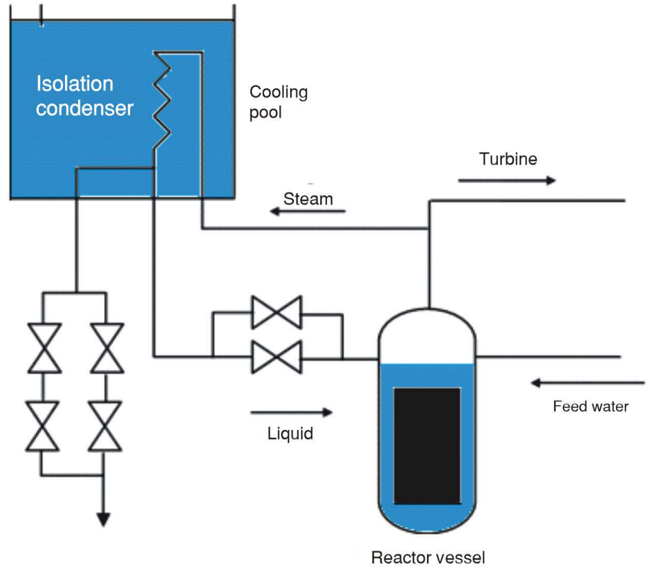

Figure 2. The ICS coupled with the primary system in BWR [19]

Table 1. Condenser type and coupling method of the PRHRS

Reactor	Electric power [MWe]	Type	Coupling	Condenser	System name
APR+	1500	PWR	SG	Slightly inclined tube	Passive auxiliary feedwater system [20]
Advanced PWR (APWR+)	1700	PWR	SG	–	Passive core cooling system using steam generator
HPR1000	1090	PWR	SG	Vertical tube	Emergency PRHRS [18]
CPR1000	1080	PWR	SG	Vertical tube	Emergency PRHRS [21]
ESBWR	1520	BWR	Primary loop	Vertical tube	Isolation condenser system
VVER-1200	1198	PWR	SG	Vertical tube	SG passive heat removal system
SWR1000	1250	BWR	Primary loop	Slightly inclined tube (as in Gundremmingen NPP)	Emergency condenser system [22]
SMART	100	Integral PWR	SG	Vertical tubes	PRHRS [23]
IRIS	335	Integral PWR	SG	Horizontally arranged U tubes	Passive emergency heat removal system [24]
CAREM	27	Integral PWR	Primary loop	Inclined tubes	PRHRS [25]
NuScale	50	Integral PWR	SG	Vertical tubes	Passive decay heat removal system [26]

Passive containment cooling system

During the loss of coolant accident (LOCA) and main steam line break (MSLB), high-pressure steam discharges into the containment and increases room temperature and pressure sharply [27]. The PCCS task is to condense the steam and control the containment pressure below the design limit. It plays a vital role in long-term cooling as the condensate is recirculated into the reactor vessel to cool the core.

Various cooling approaches such as: wall condensation, condenser tubes, suppression pools, and water spray systems are used in the reactor. Figure 3(a) and 3(b) show a schematic of PCCS exploiting containment walls as in 3(a) the AP1000 [7], the CAP1400 [9], and 3(b) the NuScale reactors [26]. Figure 3(c) shows condenser tube located in the reactor building is used for cooling in the iPOWER reactor [27-29]. For other designs, tab. 2 presents the type of condensation surface of the PCCS in various reactors.

CONDENSATION STUDIES FOR REACTOR SAFETY SYSTEM

Condensation occurs when vapor encounters a surface having a temperature lower than its saturation point. When the condensate does not wet the surface, a drop-wise mode occurs, and the liquid is in the form of droplets. A film-wise happens when the condensate is forming a thin layer. The dropwise is preferred due to a higher heat rate. However, it is challenging to practically achieve it. Hence, the design is mostly under the assumption of filmwise.

Theoretical film condensation at an isothermal vertical plate of a pure, stationary, saturated vapor was first solved by Nusselt in 1916. The formula was approached using the fundamental law of mass conservation, Newton's second law of motion, and the first law of thermodynamics with several simplifying assumptions.

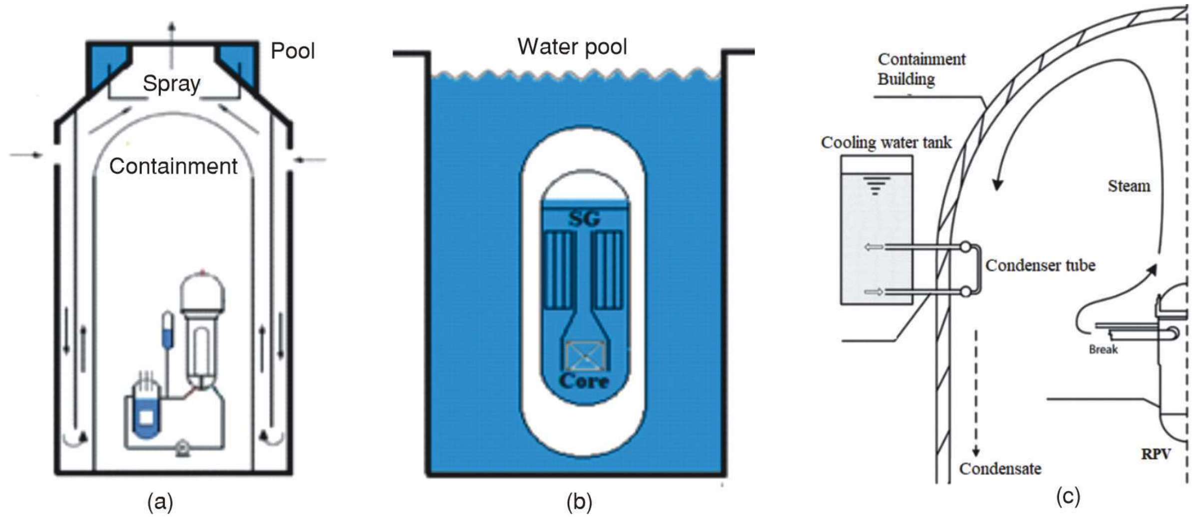

Figure 3. Passive containment cooling system [4]

Table 2.The PCCS Condensation surface in various reactors

Reactor	Electir power [MW]	Type	Condensation surface
ESBWR	1520	BWR	Inner of vertical tube [30]
iPOWER	1250	PWR	Outer of vertical tube [28]
HPR1000	1090	PWR	Outer of vertical tube [5]
AP1000	1110	PWR	Inner of steel containment vessel [7]
CAP1400	1500	PWR	Inner of steel containment vessel [9]
APR+	1560	PWR	In-tube and ex-tube of the inclined tube [31]
NuScale	50	Integral PWR	Inner of steel containment vessel [26]

In practice, the empirical formula is needed to deal with specific designs and working environments, such as the presence of NC gases [32], surface micromorphology and hydrophobicity [33], high pressure and temperature, and large sub-cooling, which may affect the overall heat transfer. Hence, a reasonably accurate correlation is essential for confirming the trustworthiness of a passive safety system.

Condensation studies for passive residual heat removal system

The PRHRS with condensation inside horizontal tube

When high temperature steam travels along the cold pipeline, it goes through stages of condensation and progresses as shown in fig. 4. At the beginning, it condenses into droplets. As quantity grows the neighboring droplets unite to form an annular liquid layer around the inner surface. The layer then gets thicker and becomes a ring-shaped wavy flow. Because of gravity, most condensate accumulates on the lower position and forms a stratified shape. Far ahead, the void fraction gets lesser, so the flow regime changes. Large bubbles appear when the wave between steam and liquid grows, establishing a slug flow in a small-diameter pipe or churn-turbulent flow for a larger tube.

In such cases, information on the flow regime is essential for determining the condensation HTC. Baker introduced a general map that defined a two- phase flow map in a horizontal tube in 1954 [34]. Following that, many have been published. A more recent one was by Zhuang *et al.* [35], which came up with a pattern map appropriate for R170 that considers influences of surface tension, the viscosity of liquid, and vapor inertia.

Various models and formulations have been developed for horizontal in-tube condensation. Some are tested for their applicability in reactor accident conditions. Shabestary *et al.* [36] evaluated formulas from Chato [37], Boyke [38], Chen [39], Dobson [40], Sharma [41], Cavallini [42, 43] and Shah, shown in tab. 3. They were all compared with condensation test data of 4.5 MPa (45 bar), that is obtained from the COSMEA [44], a facility which represents a segment of the Emergency Condenser of the KERENA reactor. Here, the steam flow is 0.610 kgs^{-1} and the heat flux is

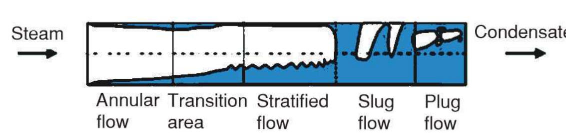

Figure 4. Condensation flow regime inside a horizontal tube [36]

Table 3. Correlations for condensation inside a horizontal tube [36]

Correlation	Reference
$$h = 0.728\varepsilon^* \left[\frac{\rho_l (\rho_l - \rho_v) g \Delta i_{lv} \lambda_l^3}{\mu_l D (T_{sat} - T_w)} \right]^{0.25}$$ $$\varepsilon^* = \frac{x}{x + (1-x)\left(\frac{\rho_v}{\rho_l}\right)^{2/3}}$$ (1) Ranges: Diameter: 14.5 mm $Re_v \leq 35\,000$ Fluid: R-113	Chato [37]
$$h = 0.024 \frac{\lambda_l}{D} Re_l^{0.8}\ Pr_l^{0.43} \frac{\sqrt{\left(1 + \frac{\rho_l - \rho_v}{\rho_v} x\right)}}{2}$$ (2) Ranges: $10.0 \leq$ Diameter ≤ 17.0 mm, 187 °C $\leq T_{sat} \leq$ 302 °C, 5.1 °C $\leq (T_{sat} - T_w) \leq$ 28.7 °C, 222 G 2240 $kgm^{-2}s^{-1}$ Fluids: R-718	Boyko and Kruzhilin [38]
$$h = 0.018 \left(\frac{\rho_l}{\rho_v}\right)^{0.39} \left(\frac{\mu_l}{\mu_v}\right)^{0.078} Re_l^{0.2} (Re_T - Re_l)^{0.7}\ Pr_l^{0.65}$$ (3)	Chen *et al*. [39]
$$h = \frac{\lambda_l}{D} \left[\frac{0.23 Re_v^{0.12}}{1 + 1.11 X_{tt}^{0.58}} \left(\frac{Ga_l Pr_l}{Ja_l}\right)^{0.25} + \left(1 - \frac{\theta}{\pi}\right) 0.0195 Re_l^{0.8}\ Pr_l^{0.4}\ \varphi(X_{tt}) \right]$$ (4) $$\varphi(X_{tt}) = \sqrt{1.376 + \frac{C_1}{X_{tt}^{C_2}}}$$ For $0 < Fr_l \leq 0.7$ $C_1 = 4.172 + 5.48 Fr_l - 1.564 Fr_l^2$ $C_2 = 1.773 - 10.169 Fr_l$ For $0.7 < Fr_1$ $C_1 = 7.242$ $C_2 = 1.655$ Ranges: $3.1 \leq$ Diameter ≤ 7.0 mm, 33.5 °C $\leq T_{sat} \leq$ 46.4 °C, 1.1 °C $\leq (T_{sat} - T_w) \leq$ 1.8 °C, $24 \leq G \leq 812$ $kgm^{-2}s^{-1}$ Fluids: R-22, R-134a, R-410A, R-32/R-125 (60-40 %)	Dobson and Chato [40]
$$h = 0.023 \frac{\lambda_f}{D} Re_l^{0.8}\ Pr_l^{0.4} (1-x)^{0.8} \left[1 + 2.164 \left(\frac{x}{1-x}\right)^{0.85} \left(\frac{P_{crit}}{P}\right)^{0.565} \right]$$ (5)	Sharma *et al*. [41]
$$h = 0.725 \left[\frac{\rho_l (\rho_l - \rho_v) g\, h_{lv} \lambda_l^3}{\mu_l D (T_s - T_w)} \right]^{1/4} \left[1 + 0.82 \left(\frac{1-x}{x}\right)^{0.268} \right]^{-1} + h_{LO} (1-x)^{0.8} \left(1 - \frac{\theta_{STRAT}}{\pi}\right)$$ (6) Ranges: Diameter: 8 mm Fluid: R-22, R-134a, R-125, R-32, R-410A	Cavallini, *et al*. [42]

Table 3. Continuation

Transition vapor velocity indicators: $$J_{\mathrm{v}}^{T}=\left\{\left[\frac{7.5}{4.3X_{tt}^{1.111}+1}\right]^{-3}+C_{T}^{-3}\right\}^{-1/3} \qquad (7)$$ where C_T = 1.6 for hydrocarbon and C_T = 2.6 for other fluids $$J_{\mathrm{v}}=\frac{xG}{[\mathrm{g}\,D\,\rho_{\mathrm{v}}(\rho_1-\rho_2)]^{0.5}}$$ The heat transfer coefficient: (a) For ΔT – independent flow regime ($J_{\mathrm{v}}^{T}<J_{\mathrm{v}}$): $$h_I=h_{LO}\left[1+1.125x^{0.8170}\left(\frac{\rho_I}{\rho_{\mathrm{v}}}\right)^{0.3685}\left(\frac{\mu_I}{\mu_{\mathrm{v}}}\right)^{0.2363}\left(1-\frac{\mu_I}{\mu_{\mathrm{v}}}\right)^{2.144}\mathrm{Pr}_l^{-0.1}\right]$$ (b) For ΔT – dependent flow regime ($J_v^T<J_v$): $$h=\left[h_I\left(\frac{J_{\mathrm{v}}^{T}}{J_{\mathrm{v}}}\right)^{0.8}-h_{\mathrm{STRAT}}\right]\left(\frac{J_V}{J_v^T}\right)+h_{\mathrm{STRAT}}$$ $$h_{\mathrm{STRAT}}=0.725\left\{1+0.741\left[\left(\frac{1-x}{x}\right)^{0.3321}\right]\right\}^{-1}\left[\frac{\lambda_l^3\rho_1(\rho_l-\rho_{\mathrm{v}})\mathrm{g}\Delta i_{lv}}{(\mu D\Delta T)}\right]^{0.25}+(1-x^{0.087})h_{\mathrm{LO}}$$	Cavallini *et al*. [43]
$$Z=\left(\frac{1}{x}-1\right)^{0.8}\mathrm{Pr}^{0.4}$$ $$h_{\mathrm{LS}}=0.023\,\mathrm{Re}_1^{0.8}\,\mathrm{Pr}_1^{0.4}$$ $$h_1=h_{\mathrm{LS}}\left(\frac{\mu_l}{14\mu_{\mathrm{v}}}\right)^{0.0058+0.557\,\mathrm{Pr}}\left[(1-x)^{0.8}+\frac{3.8\alpha^{0.76}(1-x)^{0.04}}{\mathrm{Pr}^{0.38}}\right] \qquad (8)$$ $$h_2=1.32\,\mathrm{Re}_1^{-1/3}\left[\frac{g\rho_l(\rho_l\rho_{\mathrm{v}})\lambda_l^3}{\mu_l^2}\right]^{1/3}$$ In regime I: $J_{\mathrm{v}}\geq\frac{1}{2.4Z+0.73}$ $h = h_1$ In regime II: $0.89-0.93\exp(-0.087Z^{-1.17})\geq J_{\mathrm{v}}\geq\frac{1}{2.4Z+0.73}$ $h = h_1 + h_2$ For horizontal tubes, the equation is recommended only if $\mathrm{Re_{TP}}$ > 35000 In regime II: $J_{\mathrm{v}}\leq 0.89-0.93\exp(0.087Z^{-1.17})$ $h = h_2$ Ranges: 2 ≤ Diameter ≤ 49 mm, 4 ≤ G ≤ 820 $\mathrm{kgm^{-2}s^{-1}}$, 0.01≤ x ≤ 0.99, 0.05 ≤ Z≤ 20, 68 ≤ Re_l ≤ 85 000, 0.06 ≤ J_{v} ≤ 20, 1 ≤ Pr_l ≤ 18, Fluids: water, R-11, R-12, R-22, R-32, R-113, R-123, R-125, R-134a, R-142b, R-404A, R-410A, R-502, R-507, isobutane, propylene, propane, benzene, ethanol, methanol, toluene, dowtherm 209	Shah [45]

between 850-950 $\mathrm{kWm^{-2}}$. It was found that Dobson and Chato [40] are most proper in predicting the data, while others are considerably undervalued.

The schematic of the COSMEA facility is shown in fig. 5. The test section is an annular system made from stainless steel (inner side) and titanium alloy (outer side). The inner is 43.2 mm in diameter, 2.5 mm in thickness, and 3.2 m cooled length. The facility is capable of testing up to 1 $\mathrm{kgs^{-1}}$ steam flow and the pressure range is from 0.5 MPa to 6.5 MPa. For cooling, counter-current water with a temperature of 40 Celsius and mass flow between 15-30 $\mathrm{kgs^{-1}}$ under the pressure between 0.35-0.45 MPa is used in the annulus. Wall heat flux is between 400-1100 $\mathrm{kWm^{-2}}$.

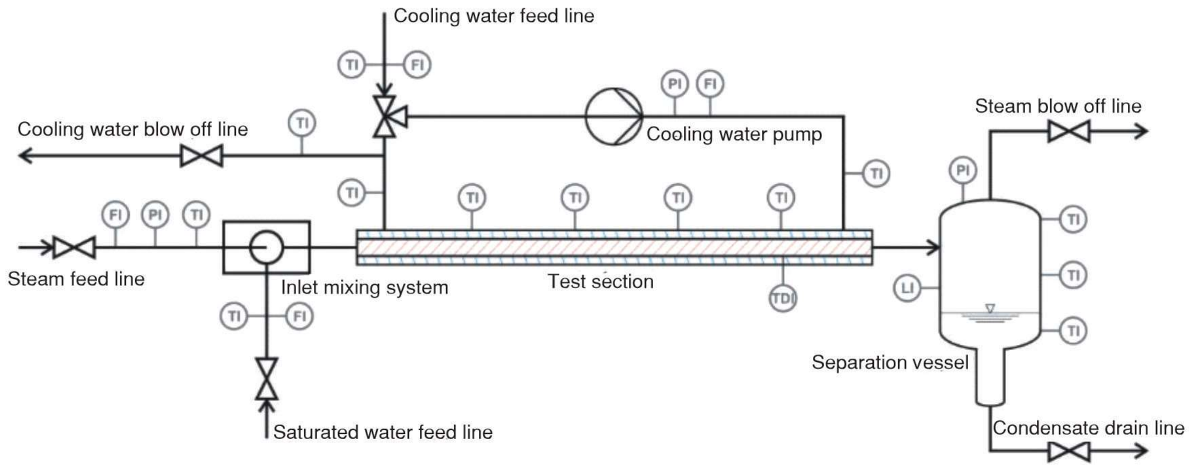

Figure 5. Schematic diagram of the COSMEA [44]

Previously, Nie *et al*. [46] evaluated the applicability of three frequently referred correlations from Akers *et al*. [47], Shah [48], and Yun *et al*. [49] shown in tab. 4. He tested condensation in a short horizontal tube of 30 cm under pressure ranging from 4 to 10 MPa that is submerged is a water tank, shown in fig. 6. Outer diameter and thickness are 25 mm and 3 mm, respectively. The mass flux is between 400 and 1000 $kgm^{-2}s^{-1}$ and steam quality ranges from 0.1 to 0.9. The study focused on the heat transfer inside the tube when pool boiling occurs outside. It was revealed that Akers's correlation has the closest prediction but is still inadequate due to the maximum deviation of –40%. A new formula was then derived from the Akers's work as follows [46]

$$\mathrm{Nu} = \frac{hD}{k_f} = 0.0312\,\mathrm{Pr}_f^{1/3}\left\{D\left[Gx\left(\frac{\rho_f}{\rho_\mathrm{v}}\right)^{1/2} + G(1-x)\right]/\mu_f\right\}^{0.8} \tag{9}$$

Table 4. In-tube steam condensation correlations evaluated by Nie [46]

Correlation	Reference
$\mathrm{Nu} = \frac{hD}{k_f} = 0.026\,\mathrm{Pr}_f^{1/3}\left\{D\left[Gx\left(\frac{\rho_f}{\rho_\mathrm{v}}\right)^{1/2} + G(1-x)\right]/\mu_f\right\}^{0.8}$ (10) For: $\left[GD\frac{(1-x)}{\mu_f}\right] > 5000 \quad \left[GDx\frac{\left(\frac{\rho_f}{\rho_\mathrm{v}}\right)^{1/2}}{\mu_f}\right] > 20000$	Akers *et al*. [47]
$\mathrm{Nu} = \frac{hD}{k_f} = 0.023\,\mathrm{Re}_{fo}^{0.8}\,\mathrm{Pr}_f^{0.4}\left[(1-x)^{0.8} + 3.8x^{0.76}\frac{(1-x)^{0.04}}{\mathrm{Pr}^{0.38}}\right]$ (11) For: $0.002 < P_R < 0.44;\ 10.8 \le G \le 1600\,\mathrm{kgm^{-2}s^{-1}};\ \mathrm{Pr}_f > 0.5;$ $0 \le x \le 1;\ \mathrm{Re}_{fo} > 350;\ 7 \le D \le 40\,\mathrm{mm};\ 3 \le \frac{G}{\rho_\mathrm{v}} \le 300\ \mathrm{ms}^{-1}$	Shah [48]
$\mathrm{Nu} = \frac{hD}{k_f} = F(0.023\,\mathrm{Re}_{fo}^{0.8}\,\mathrm{Pr}_f^{0.4})$ (12) where: $F = 0.7913 f_D f_{H0}(1-\varepsilon_\mathrm{wallis});\ f_D = [1-0.24(1-D_R)^{0.5}]^4;$ $D_R = 0.05\,\mathrm{m};\ \varepsilon_\mathrm{wallis} = (1+X_{tt}^{0.8})^{-378};\ f_H = 1+10^{-5}\,\mathrm{Re}_\mathrm{v}^{0.8};$ $X_{tt} = \left(\frac{\mu_f}{\mu_\mathrm{v}}\right)^{0.1}\left(\frac{\rho_\mathrm{v}}{\rho_f}\right)^{0.5}[(1-x)/x]^{0.9}$	Yun *et al*. [49]

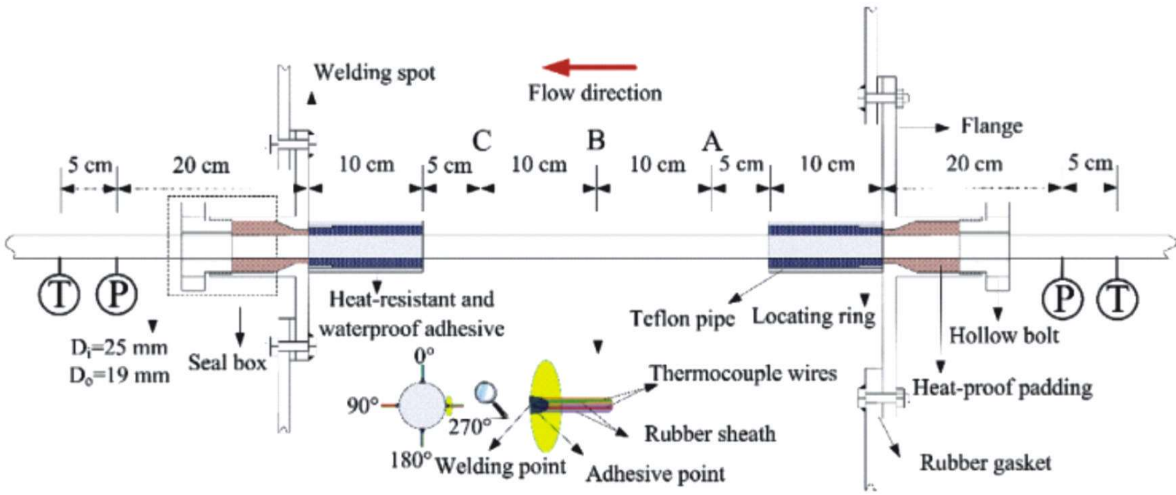

Figure 6. Test section used in Nie's experiment [46]

In addition, the work observed that the wall temperature is not uniform in the peripheral direction. The wall's heat flux and temperature increase with mass velocity, pressure, and quality of steam. The pressure drops and the HTC rises with the quality of steam and mass velocity but falls with pressure.

Another investigation on horizontal PRHRS was performed by Xu *et al*. [50] that focused on the impact of wall sub-cooling on three different flow regimes; annular, wavy, and stratified flow. Water-cooled and air-cooled surfaces were used on the outer. The schematic for water cooled system is shown in fig. 7. The test section is made of SS304 with 1.5 m effective length. The outer diameter and thickness are 28 mm and 1.5 mm, respectively. During the experiment, the velocity of the gas-steam mixture, NC gas mass fraction, and system pressure are varied to learn their impacts on the HTC. It was detected that in the stratified flow, local HTC declines with the increase of wall sub-cooling. However, the opposite condition occurs in the annular and wavy flow regimes where the HTC increases. Xu proposed a modified correlation based on his previous work [50] and Liu *et al.* [51] as follows

$$\mathrm{Nu} = 0.266 W^{-0.252}\, \mathrm{Re}_m^{0.552}\, P_{\mathrm{sred}}^{0.415}\, f(\mathrm{Ja}) \quad (13)$$

For annular and wavy flow

$$Ln\, f(\mathrm{Ja}) = -1.37 - 0.644 Ln\,\mathrm{Ja} + \\ +[-1.713 + 0.11\, Ln\,\mathrm{Re}_m + 0.02\, Ln\, W - 0.2\, Ln\, P_{\mathrm{red}} - \\ -0.008\,(Ln\, j^{+} \times 10^{-4})]\, Ln\,\mathrm{Ja}^2 - 0.113\, Ln\, Ja^3 \quad (14)$$

For stratified flow

$$Ln\, f(\mathrm{Ja}) = -1.37 - 0.644 Ln\,\mathrm{Ja} + \\ +[-1.713 + 0.11\, Ln\,\mathrm{Re}_m + 0.02\, Ln\, W - 0.2\, Ln\, P_{\mathrm{red}} - \\ -0.008\,(Ln\, j^{+} \times 10^{-4})]\, Ln\,\mathrm{Ja}^2 - 0.157\, Ln\,\mathrm{Ja}^3 \quad (15)$$

Valid for

W = 5.18-67.46 %; Re_m = 6748-61,704; wall sub-cooling ΔT = 5.92-77.26 K, inlet pressure p = 0.071-0.4 MPa.
where W is the mass fraction of local NC gas, Re_m – the Reynold's number of steam-gas mixture, P_{sred} – the ratio of the partial *vs*. the critical pressure of steam, and f (Ja) – the function that expresses the wall sub-cooling effect.

The new correlation provides a relative error within 20 % when compared with experiment results.

The PRHRS with condensation inside inclined tube

Some PRHRS are of inclined tube condensers. Cho *et al*. [20] verified four existing correlations for a slightly inclined tube of the APR+ PAFS condenser design. They are: the Shah model formulated in 1979 [48], the Thome correlation [52], the updated Shah formula for an inclined or vertical tube, and the improved Shah formula for a horizontal pipe [52]. For calculation, these formulas were integrated into the MARS code. Their results were compared with data gathered from the PASCAL facility at operating conditions of 7.4 MPa and 290 °C. The work shows that Thome's model is most appropriate for simulating the overall thermal performance of the PAFS. The PASCAL facility and the nodalization of the MARS code in the analysis are shown in fig. 8.

Meanwhile, Amidu *et al.* [53] investigated the effect of tube slope on thermal performance, figs. 9 and 10. A single-tube heat exchanger submerged in a water pool is analyzed using a combination of two thermal-hydraulic codes. The CUPID code is for the outer

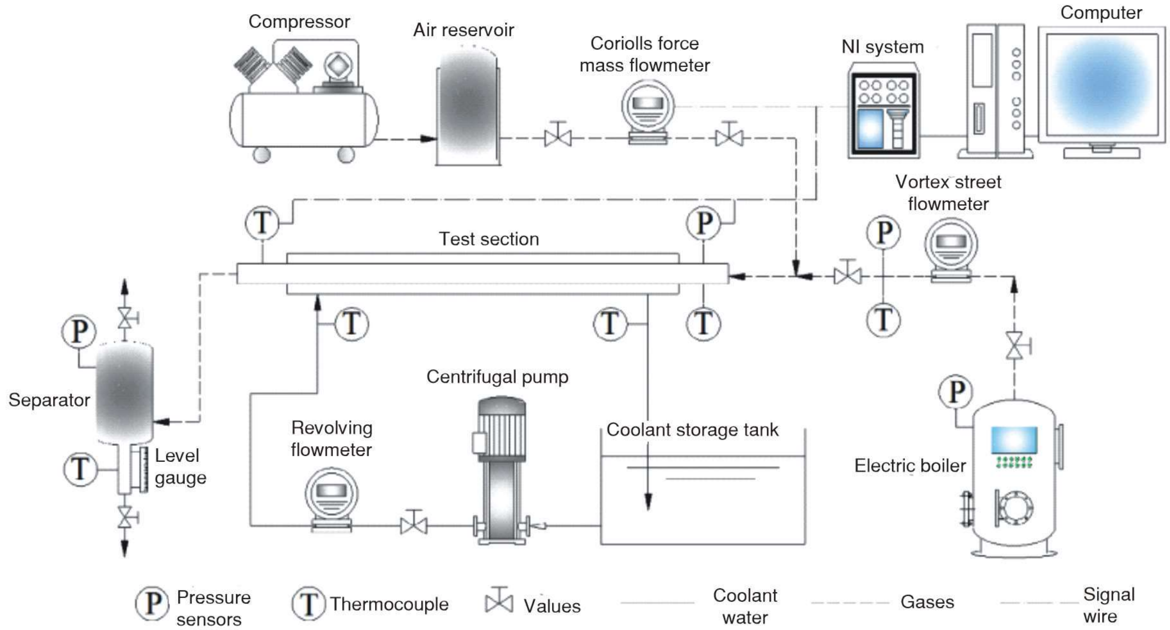

Figure 7. Xu's [50] apparatus for experiment with a water cooling system

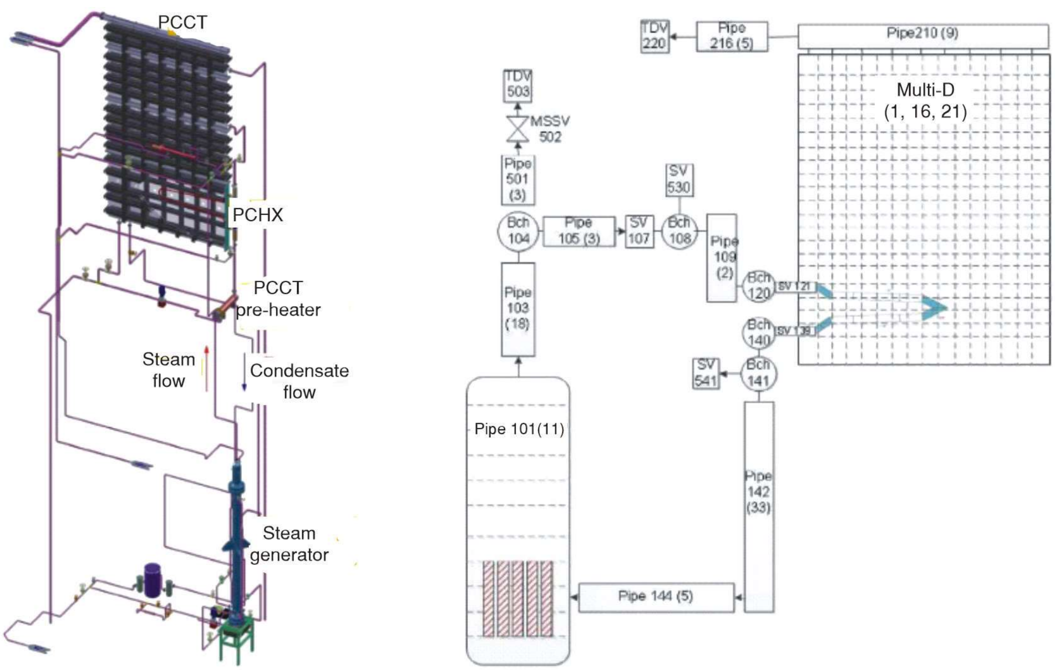

Figure 8. (a) PASCAL facility and (b) MARS nodalization [20]

side, and the MARS code is for the inner side. The steam inlet is saturated at 0.4 MPa, and the boiling pressure is at 0.1 MPa. The calculation is then validated using reference data of 30° angles.

Simulations were performed with angles ranging from 3° to 90°. It was revealed that the thermal performance is not significantly affected by the inclination. Amidu *et al.* [53] indicated that an increase in the angle causes a reduction in boiling heat transfer coefficients. However, this effect is compensated by an increase in condensation HTC due to accelerated condensate liquid film inside the tube.

Likewise, Abadi and Meyer [54] also performed coexisting condensation and pool boiling simulations using the ANSYS Fluent 17.1 package, fig. 11. The steam is at a saturated temperature of 250 °C and mass flux of 100-400 kgm^{-2}s^{-1}, with quality varied between 0.2 and 0.8. The pool saturated temperature is 100 °C. It was observed that the heat transfer coefficient rises with the increase in quality and mass flow rate. Al-

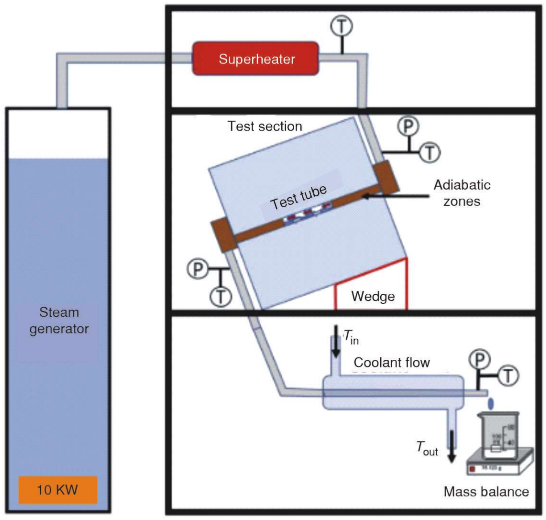

Figure 9. Schematic of Amidu's experiment [53]

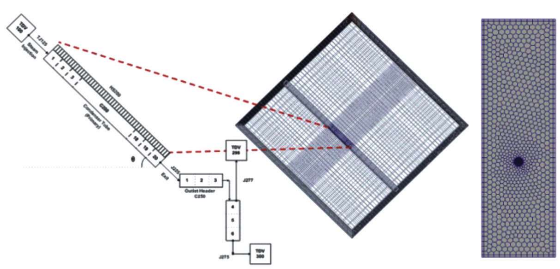

Figure 10. The computational approach in Amidu's work [53] (a) Nodalisation in MARS code (b) Meshing in CUPID for the pool

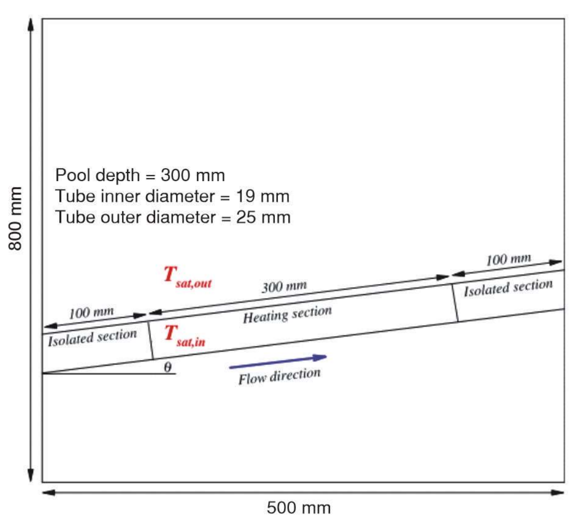

Figure 11. The model used in Abadi and Meyer's work [54]

though there is no clear tendency for the angle's influence, it was noticed a slightly higher value of the total HTC at the angle between $\theta = -60°$ and $\theta = -30°$.

The PRHRS with condensation inside a vertical tube

For PRHRS using vertical tubes, shown in tab. 1, numerical simulations were performed by Rao *et al*. [55] to learn the applicability of the existing pure steam vertical in-tube condensation model (PSVCM). Under the RELAP5 code, six combinations are simulated. They are grouped into; three models, modified UCB [56], Oh [57], and Lee and Kim [58] for laminar and two models. Shah [48] and Kim [59], for turbulent conditions. The schematic of the test facility, nodalization in RELAP5, and calculation matrix are shown in fig. 12 and tab. 5. Simulation results showed that the combination of the Oh model and Kim model provides the best prediction of the experimental results compared to the other combined models.

Other work on vertical tubes was done by Kim and No [59] which examined the influence of the inner tube diameter. The experiment used a 1.8 m long stainless 316 tube with 46 mm ID, and steam pressure up to 7.5 MPa, referring to the KNGR/APR1400 and the SBWR designs. The tube is submerged in a water pool at atmospheric pressure, shown in fig. 13. An analytical model based on the similarity of the heat transfer mechanism between the single-phase turbulent convection and the annular turbulence film condensation was developed.

The proposed correlation for the film flow is as follows [59]

$$h_2 = \frac{f_D}{(1-a)} \mathrm{Re}_2^{0.8} \mathrm{Pr}_f^{0.4} \frac{k_f}{D} \tag{16}$$

$$\mathrm{Re}_2 = \frac{\rho_f \alpha_f v_f D}{\mu_f} \tag{17}$$

The f_D is the factor that takes into account the effect of tube diameter on film condensation and is empirically formulated as follows [59]

$$f_D = 0.0182[1-0.24(1-4.47D^{0.5})]^4 \tag{18}$$

The void fraction of the flow is defined in terms of the Martinelli parameter [59]

Table 5. Calculation matrix in Rao's work [55]

Group	Turbulent model	Laminar model
PSVCM1	Shah [48]	Nusselt
PSVCM2	Shah [48]	Mod. UCB
PSVCM3	Kim [59]	Mod. UCB
PSVCM4	Shah [48]	Oh [57]
PSVCM5	Kim [59]	Oh [57]
PSVCM6	Shah [48]	Lee and Kim [58]
PSVCM7	Kim [59]	Lee and Kim [58]

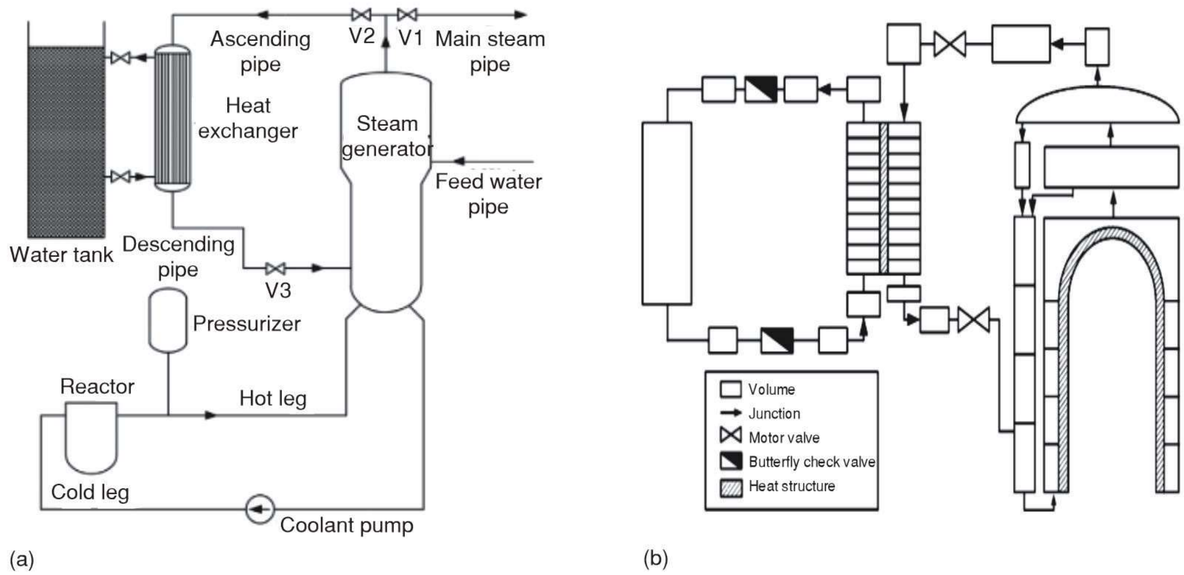

Figure 12. (a) Schematic of the test facility and (b) RELAP5 nodalization [55]

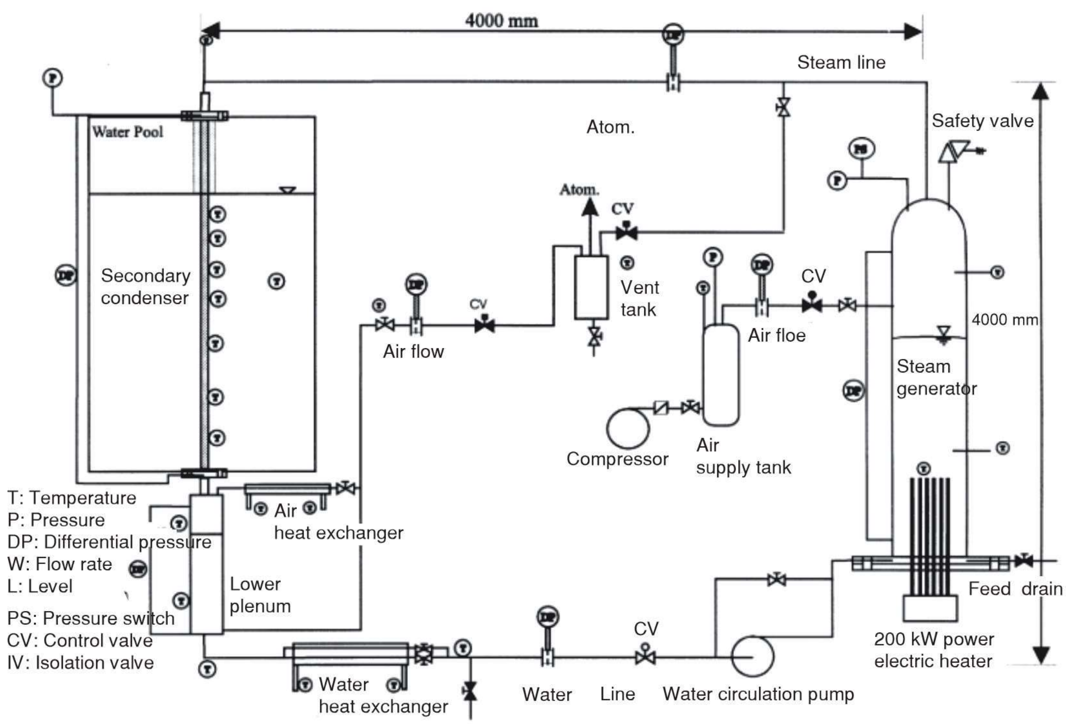

Figure 13. Schematic of Kim's test apparatus [59]

$$\alpha = (1 + X_{tt}^{e_1})^{e_2} \tag{19}$$

$$X_{tt} = \left(\frac{\mu_l}{\mu_v}\right)^{0.25} \left(\frac{1-x}{x}\right)^{1.75} \left(\frac{\rho_v}{\rho_l}\right) \tag{20}$$

The factors of e_1 and e_2 are selected as 0.6, and 0.15, respectively, from the experimental data. The correlation is valid for tube diameter in the range of 7.4 to 50 mm. The formula is then compared with the model proposed by Shah [48]. The newly developed correlation provides better estimation when associated with the experimental data.

Other research was conducted by Chung *et al*. [60], which performed up to 6 MPa, the pressure of the SMART reactor's HX operating range. Chung et al. [60] proposed a modified correlation based on Lee and Kim [61, 62]. The new correlation for both pure steam conditions and a mix of steam gas is as follows.

For pure steam

$$h_{\text{Modified-Lee}} = 1.03 \cdot \tau_g^{0.15} \cdot h_{\text{Nusselt}} \tag{21}$$

$$\tau_g = \frac{\frac{1}{2}\rho_g u_g^2 f_R}{\text{g}\,\rho_f L} \tag{22}$$

$$L = \left(\frac{v_f^2}{\text{g}}\right)^{1/3} \tag{23}$$

$$h_{\text{Nusselt}} = \frac{k_l}{0.9086}\left(\frac{\mu_f^2 \,\text{Re}_f}{\text{g}\,\rho_f \Delta\rho}\right) \tag{24}$$

$$f_R = \begin{cases} 0.079\,\text{Re}_g^{-1/4} & \text{for Re} > 2300 \\ 16/\,\text{Re}_g & \text{for Re} > 2300 \end{cases}$$

where τ_g represents non-dimensional shear stress, which is influenced by the degradation factor of the steam f_R and characteristic length scale L.

The h_{Nusselt} is the Nusselt formulation for the heat transfer coefficient of condensation.

For the steam-gas mix

$$h_{\text{KSP}} = f_1 f_2 h_{\text{Nusselt}} \tag{25}$$

where f_1 is a pure steam factor which is determined from the Reynolds number and film thickness. Meanwhile, the f_2 represents the NC gas effect, which depends on the mass of the gas

$$f_1 = (1 + 7.3210^{-4}\,\text{Re}_f)\left(\frac{\delta_f}{\delta_{f,o}}\right) \tag{26}$$

where δ_f and $\delta_{f,o}$ are the film thickness without and with interfacial shear stress

$$f_2 = \begin{cases} 1 - 2.601 W_{nc}^{0.708} & \text{for } W_{nc} < 0.1 \\ 1 - W_{nc}^{0.292} & \text{for } W_{nc} > 0.1 \end{cases} \tag{27}$$

The correlation was then evaluated using data from two laboratories, the University of California at Berkeley and Pohang University of Science and Technology, South Korea. It shows that for the pure steam, the correlation predicts well within 25 %, and for the steam-air mixture, it under-predicts by less than 25 %.

Condensation studies for passive containment cooling system

Reactor containment has three safety functions: to confine radioactive materials, to protect against external hazards, and as radiation shielding [63]. Its integrity is crucial to avoid radioactive release. A condensation approach as a mechanism to reduce pressure is implemented.

In PCCS, condensation may occur on the HX's outer tube or the inner wall of the containment vessel, shown in fig. 3. Since the containment is full of air during normal operation, NC gas presence should be considered. Studies on these are as follows.

The PCCS with condensation on the outer surface of the vertical tube

Investigation on a vertical cylinder outer surface condensation was performed by Lee, *et al*. [64]. The test cylinder was a 1 meter length and 40 mm O. D. pipe, shown in fig. 14. The influence of air mass fraction and pressure for the air and the steam mixture under natural convection is studied, with exact control of wall subcooling. The study revealed that heat transfer is notably affected by the strength of natural convection movement that is represented by the Grashof number. A dimensionless empirical correlation is proposed based on the regression of in-house test data and from Dehbi's experiment [65]. The correlation is as follows [64]

$$\text{Nu}_D = 890\,\text{Gr}_L^{0.125} W_s^{*0.966}\,\text{Ja}^{-0.327} \tag{28}$$

were

$$W_s^* = 1 - W_a^{0.01} \tag{29}$$

The formula is valid for the tube length between 1.0 m to 3.5 m, the Grashof number of $1.3\cdot 10^{10} \le \text{Gr}_L \le 5.05\cdot 10^{12}$, the steam mass fraction of $1.16\cdot 10^{-3} \le W_s^* \le 2.35\cdot 10^{-2}$ and Jacob number of $0.009 \le \text{Ja} \le 0.035$.

In line with that, Fan *et al*. [66] also performed an experiment using a vertical tube under free convection, shown in fig. 15. The test section was a smooth stainless-steel pipe with an outer diameter of 31.1 mm and a length of two meters. A large number of 374 data sets were collected to unravel the complex dependency between pressures, wall sub-cooling, and air mass fraction. Fan revealed that the HTC decreases with the wall sub-cooling increase, which depends on the wall sub-cooling itself and the total pressure. Fan *et al.* also proposed a condensation HTC is as follows [66]

$$h = \frac{[(32021 - 22766P) + (-16107 + 11736P)\log(100 W_a)]}{\Delta T^{(0.561 + 0.00134\Delta T - 0.546P)}} \tag{30}$$

The formula is valid for pressure between 0.2 MPa to 0.5 MPa, air mass fraction of $0.10 < W_a < 0.8$, and subcooling temperature of 10 °C < ΔT < 70 °C. It is claimed that the correlation is applicable not only for air but also for other NC gases (nitrogen and argon) after comparing with test data from other works, Uchida *et al.* [67], Su *et al.* [68], Anderson [69], and Kim *et al.* [70]). The mean error is around 7 %, and about 96 % of the test data deviation is within 20 %.

Complementing the single tube studies, an investigation to clarify the effect of tube bundling was performed by Bae *et al*. [8] using the CLASSIC facility. The work was primarily to clarify the performance of the iPOWER's containment cooling system. The heat transfer for both a single tube and a bundle of eighteen vertically arranged tubes was analyzed, shown in fig. 16. New correlation for the single tube

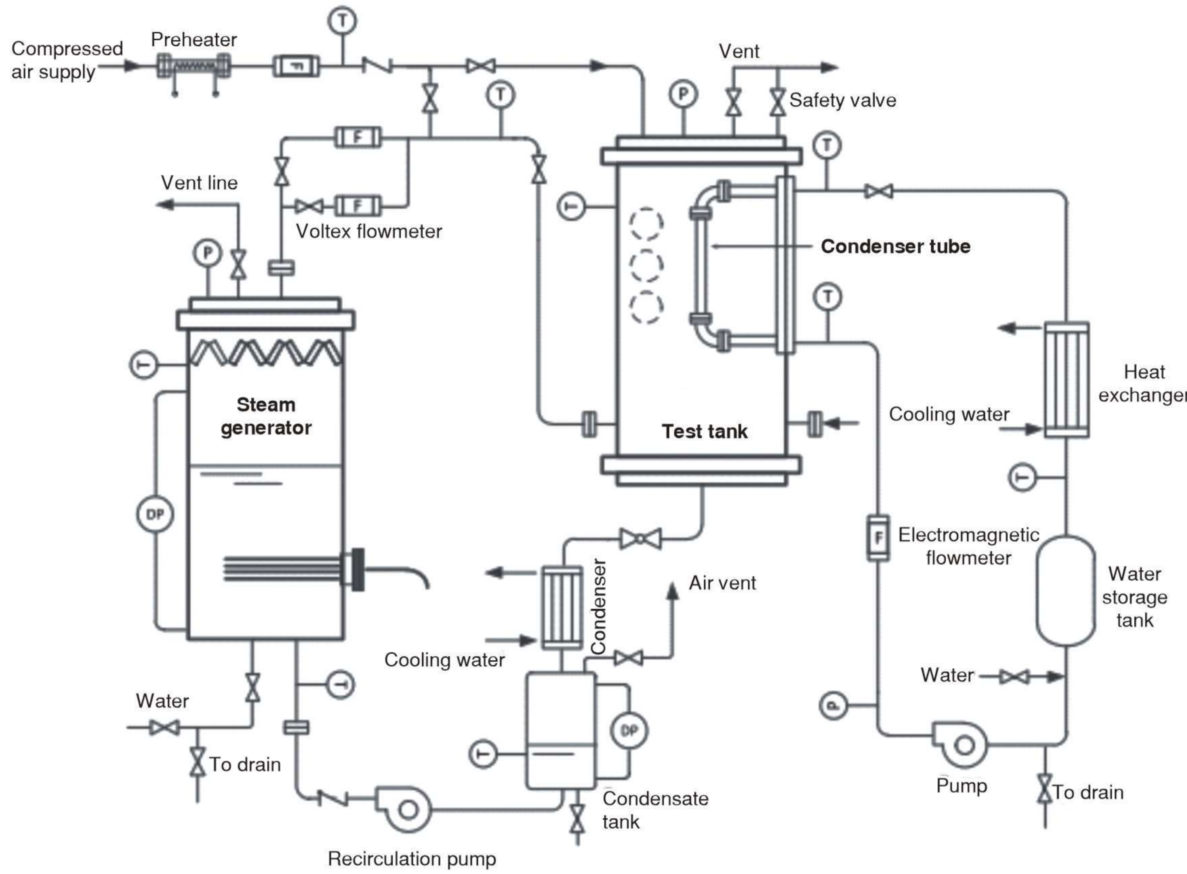

Figure 14. Schematic diagram of test system [64]

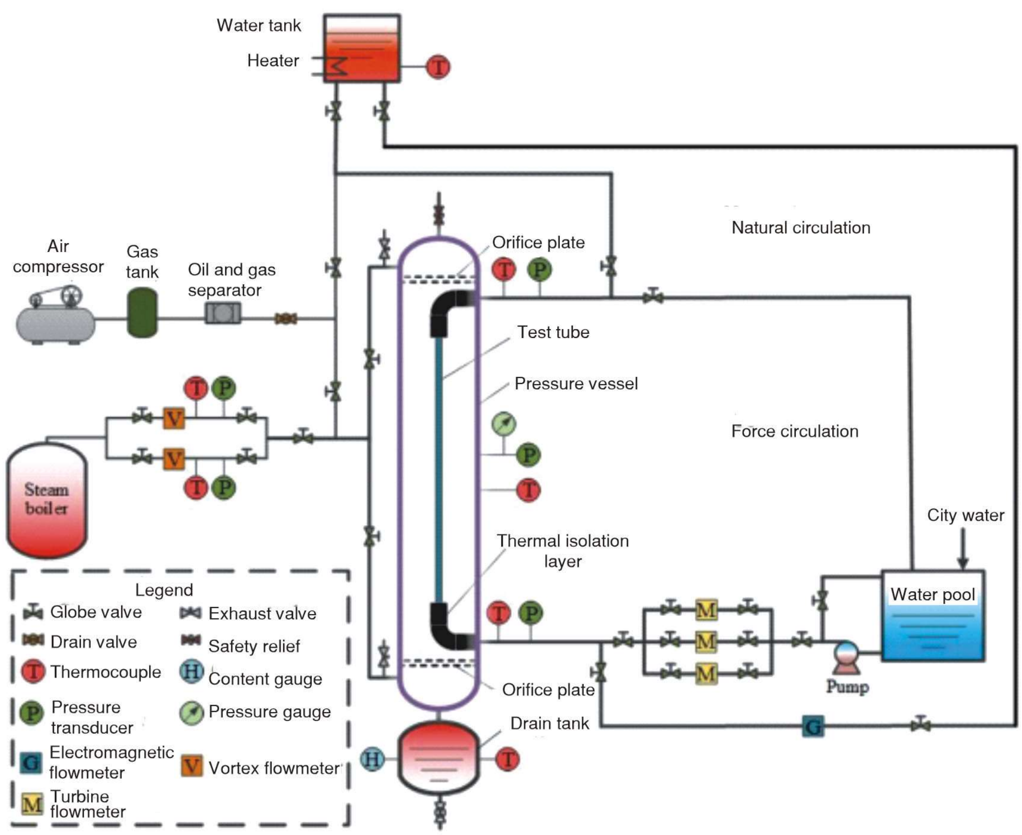

Figure 15. Schematic of Fan's experimental system [66]

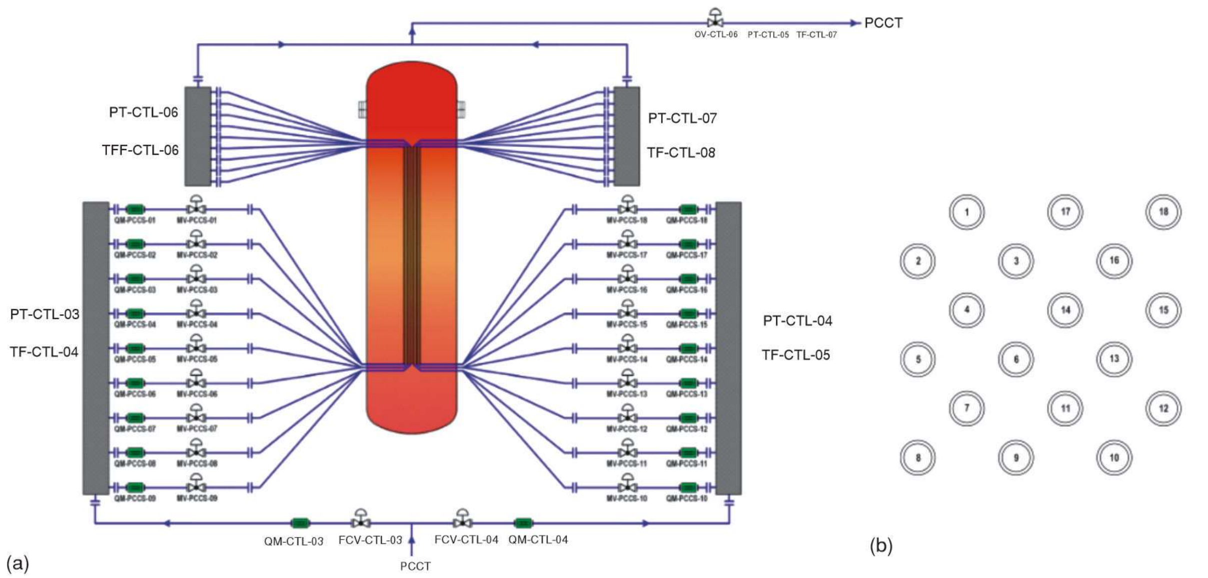

Figure 16. (a) Coolant circulation diagram and (b) bundle tube layout of Bae's work [8]

was proposed by revising the curvature effect and the free parameter of Dehbi's model [71]. This modification was made due to a longer tube in the CLASSIC facility (5 m) than used by Dehbi (3.5 m). This study also suggested a new practical free parameter (φ) based on the Bird correction factor. The proposed correlation in terms of the Nusselt number is as follows

$$\mathrm{Nu}_{\mathrm{PCCS}} = \varphi_{\mathrm{PCCS}} \left(\frac{\mathrm{Nu}_{\mathrm{cyl}}}{\mathrm{Nu}_{\mathrm{flat}}} \right)_{\mathrm{PCCS}} \mathrm{Nu}_{\mathrm{HMTA}} \tag{31}$$

where

$$\varphi_{\mathrm{PCCS}} = 1.08 \cdot \theta^{0.53} \tag{32}$$

$$\left(\frac{\mathrm{Nu}_{\mathrm{cyl}}}{\mathrm{Nu}_{\mathrm{flat}}} \right)_{\mathrm{PCCS}} = 1.25 \tag{33}$$

$$\mathrm{Nu}_{\mathrm{HMTA}} = 0.13 g^{1/3} D^{2/3} \frac{d}{k} \left(\frac{\rho_{\mathrm{w}} + \rho_{\mathrm{b}}}{2} \right) \left(\frac{\rho_{\mathrm{w}} - \rho_{\mathrm{b}}}{\mu} \right)^{1/3} \left(\frac{w_{\mathrm{s,b}} + w_{\mathrm{s,w}}}{1 - W_{\mathrm{s,w}}} \right) \left(\frac{h_{fg}}{T\mathrm{b} - T_{\mathrm{w}}} \right) \tag{34}$$

A consistent average heat transfer coefficient was observed in bundle analysis compared to the single tube model. However, a local heat transfer degradation occurred in the inner tubes due to the NC gas accumulation. The average factor of this shadow effect is approximately 0.939. Bae suggested to consider this effect in determining the dimension of PCCS.

The PCCS with condensation on the downward surface

Double containment design where the inner part is a metal vessel, and the outer is a concrete structure has been implemented in the AP1000 and CAP1400 reactors shown in fig. 3(a). The challenge to accurately predict condensation heat transfer at the downward-facing surface arises due to complex phenomenon underneath.

To clarify that, Chen *et al*. [9] investigated steam condensation on the surface below a horizontal plate to evaluate the CAP1400 containment upper dome. The test surface was a stainless-steel plate coated with 0.08 mm inorganic zinc as in the actual vessel. Figure 17 shows a schematic of the test facility. The steam-air mixture is varied with pressure between 0.154 MPa and 0.607 MPa, molar fraction of air between 1.1 % and 82.9 %, and wall sub-cooling between 12.6 °C and 49.3 °C.

The experimental results were used to assess four correlations from Uchida *et al*. [67], Tagami [72], Dehbi [65], and Liu [51] *et al*. shown in tab. 6. It was discovered that all significantly overestimated the condensation heat transfer coefficient on the test data.

Chen then proposed empirical condensation HTC developed using the least square fitting method [9]

$$h = 622.48 P_{\mathrm{b}}^{0.325} \Delta T_{\mathrm{s}}^{-0.391} 0.0713^{X_a} \tag{39}$$

where P_{b} [kPa] is the bulk pressure, ΔT_s [°C] – the wall sub-cooling temperature, and X_a – the molar fraction of air.

It was reported that all the test data could be estimated within ±25 % error

RESEARCH GAP

From the previous discussion, most of the recent studies on safety systems addressed straight tube ge-

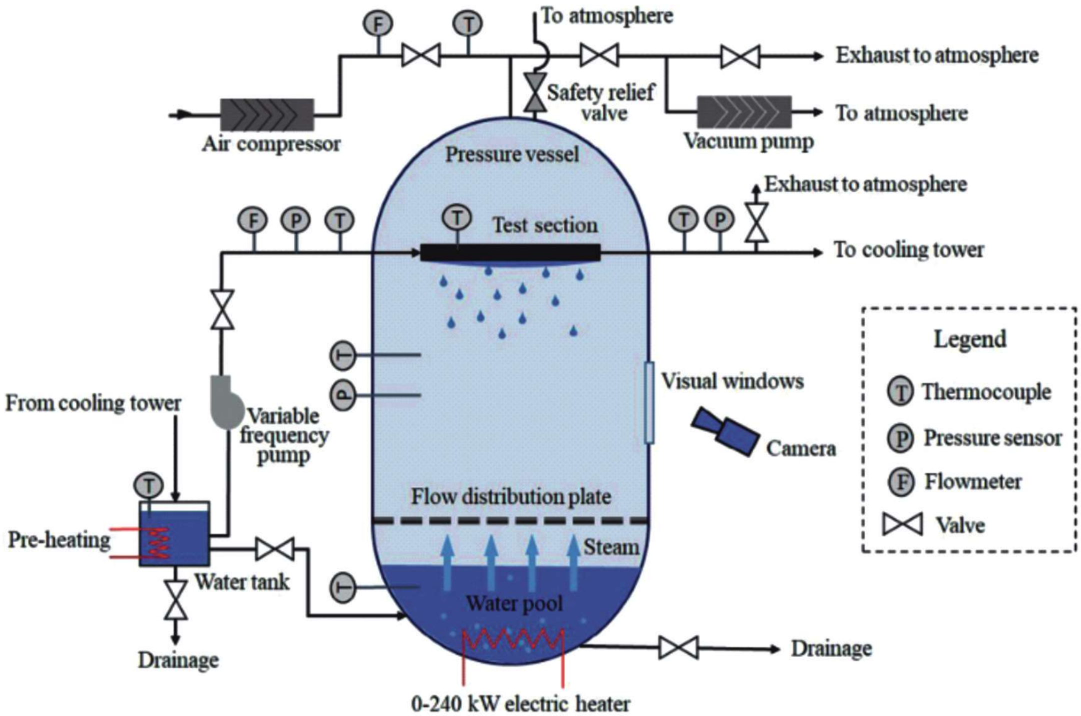

Figure 17. Schematic of the test facility of Chen's work [9]

Table 6. Four correlations evaluated by Chen [9]

Reference	Correlation	Conditions
Uchida *et al*. [67]	$h = 380\left(\frac{W_a}{W_v}\right)^{-0.7}$ (35)	$0.23 \le W_a \le 0.91$ $0.1 \le P \le 1.8$ MPa $10 \le \Delta T \le 140$ K $0.3 \le L \le 0.9$ m
Tagami [72]	$h = 380\left(\frac{W_a}{W_v}\right)^{-0.7}$ (36)	$0.38 \le W_a \le 0.83$ $T_w = 322$ K $L = 0.3$ m
Dehbi [65]	$h = \frac{L^{0.05}[(3.7+28.7P_b)-(2438+458.3P_b)\log W_a]}{\Delta T_s^{0.25}}$ (37)	$0.28 \le W_a \le 0.9$ $0.15 \le P \le 0.45$ MPa $10 \le \Delta T \le 50$ K $0.3 \le L \le 0.35$ m
Liu *et al*. [51]	$h = 55.635 X_v^{2.344} P_b^{0.252} \Delta T_s^{0.307}$ (38)	$0.395 \le X_s \le 0.873$ $0.25 \le P \le 0.46$ MPa $4 \le \Delta T \le 25$ K

ometry (vertical, horizontal, and inclined) and downward-facing surfaces of large vessels. They have not so far investigated helical geometry as there is no such model of the PRHRS and PCCS in existing reactor designs.

Several new integral reactor designs have come with helical SG, such as the CAREM, IRIS, SMART, and NuScale reactors. During normal operation, the SG is to produce superheated steam. However, when an accident occurs it has the potential to function for cooling down the primary system. Hence it is valuable to further investigate this capability.

One of the reactor designs shown in fig. 18(a) places its module in a water pool. When LOCA occurs the ECCS passively cools the reactor by opening several valves. Steam that comes out from the upper valves, condenses on the containment wall. The condensate will be re-injected into the reactor vessel through the lower valves shown in fig. 18(b). The effectiveness of this system has been confirmed by Skolik *et al*. [73].

If the ECCS fails the reactor could end up with a core damaged [74], as the decay heat cannot be removed. A possible solution to rescue is by using the SG [75]. Supplying cold water into the feedwater line would change the role of SG into a cooling condenser as the shell side is occupied with saturated steam shown in fig. 18(c).

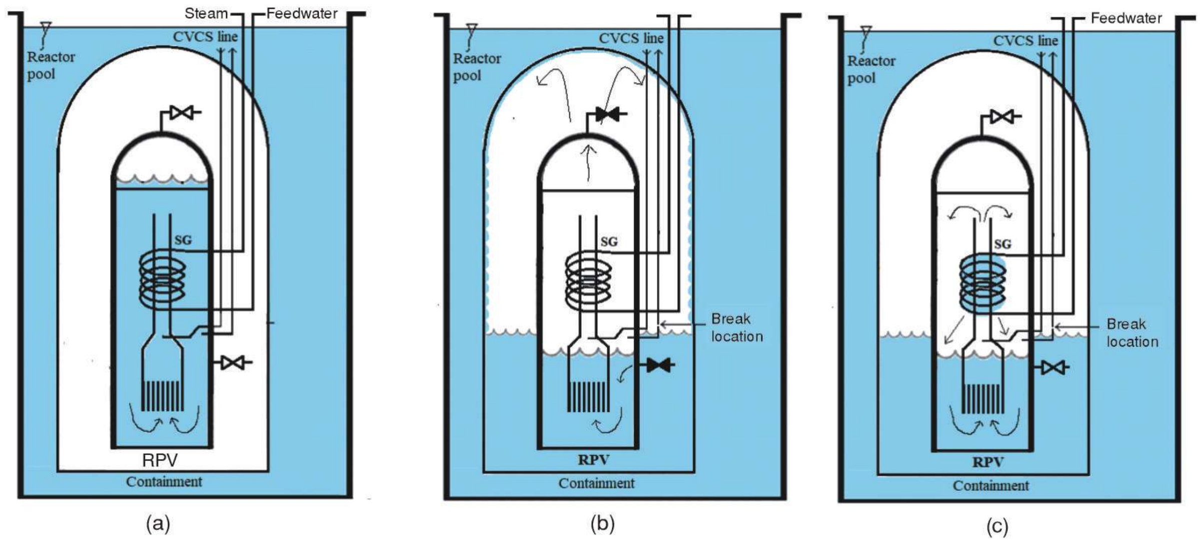

Figure 18. Schematic of Integral SMR (a) Normal operation, (b) Cooling using ECCS, and (c) Cooling using SG

The effectiveness of this approach needs further investigation because the SG is not originally designed for that. One of the parameters to be confirmed is the condensation HTC as the SG has a specific design that is not commonly found in other industries. Its geometry is tall and consists of many stacked tubes and a large helical diameter.

Under high pressure circumstances and specific geometry conditions, the validity of the existing condensation formula needs to be clarified. The work on this is essential to precisely confirm whether the helical SG has enough capacity to play a role as a cooling condenser during accident mitigation action.

So far, studies on the use of SG for cooling post a LOCA in PWR are mostly dealing with condensation inside vertical tubes. This is the case because conventional reactor design uses an inverted *U*-tube. A study for the helical tube SG which plays a role as a cooling condenser post a LOCA has never been conducted. Future study in this area is important to ensure the safety of integral reactors having helical coil SG as part of accident management.

CONCLUDING REMARKS

The Fukushima accident reveals that passive features are crucial in nuclear reactors. Some PRHRS and PCCS designs have been explored in this paper. Design variation among the condensers is identified and correlations suitable for accident conditions derived from experimental are presented.

For PRHRS with horizontal tube condensers, a study by Shabestary *et al*. [34] shows that Dobson's model is most suitable for high-pressure steam inside a large tube among eight correlations under investigation. Meanwhile, Nie *et al*. [46] observed heat flux and wall temperature increase in proportion to steam quality, pressure, and mass velocity and proposed a correlation derived from Akers's work. Another work by Xu *et al*. [50] found that in a stratified flow regime, local HTC declines with the increase of wall sub-cooling, but in annular and wavy flow regimes, the HTC increases. Xu *et al*. [50] proposed modified correlations for three flow regimes.

Using computer codes, Amidu *et al*. [53] indicated that the thermal performance of the condenser is not significantly affected by the tube inclination angle. Meanwhile, Abadi and Meyer [54] spotted that a slightly higher heat transfer was observed when the angle is in the range of $\theta = -60°$ to $\theta = -30°$. With MARS code Cho *et al*. [20] found that the Thome model provides the best estimation among the four correlations tested using data derived from the PASCAL facility.

For PRHRS with a vertical tube, Kim and No [59] develop a new correlation for a large tube based on heat transfer mechanism similarity between the single-phase turbulent flow and the annular film condensation flow inside a tube. Meanwhile, Chung *et al*. [60] proposed correlations between pure steam and a steam-gas mixture, a modification of previous work by Lee and Kim [62].

A study of the PCCS performance was performed by Lee, Jang, and Choi [64] for the air-steam mix condensation on a vertical tube's outer surface case. They suggested considering the Grashof number. Meanwhile, Fan *et al*. [66] also developed a correlation for turbulent free-convection in the presence of air. Concerning bundle configuration, Bae *et al.* [8] pointed out that heat transfer degradation due to the shadow effect of other surrounding tubes should be considered. For PCCS utilizing the containment wall as a condensing surface, Chen *et al*. [9] studied the HTC on the upper part of the containment. He offered a new correlation after evaluating the suitability of several existing correlations.

It appears that several acknowledged correlations require tunning to be implemented in the passive safety system. Some new correlations have been proposed to cover the specifics of condenser design and reactor accident conditions. Lastly, future study on condensation on the outer surface of the helical coil is necessary to assess the possibility of the integral reactor's SG changing role as a cooling condenser post a LOCA that is followed by safety system failure.

ACKNOWLEDGMENT

The authors are thankful for the support from Universitas Indonesia under the grant scheme of seed funding professor FTUI year 2022. Contract number NKB-1956/ UN2.F4.D/PPM.00.00/2022.

NOMENCLATURE

- D Diameter [m]
- Fr Froude number
- g Gravitational acceleration, 9.81 [ms^{-2}]
- G mass velocity [kgm^{-2}s^{-1}]
- Ga Galilei number $Ga_l = g\rho_l(\rho_l - \rho_v)D^3/\mu_l$ in eq. (4)
- h Heat transfer coefficient [Wm^{-2}K^{-1}]
- h_{LO} Heat transfer coefficient (liquid only) $h_{LO} = 0.023\ Re_l^{0.8}\ Pr_l^{0.4}(\lambda_l / D)$ [Wm^{-2}K^{-1}]
- Ja Jakob number $Ja_l = Cp_l(T_s - T_w)/H_{evap}$ in eq. (4)
- J_v^T Transition dimensionless gas velocity eq. (7)
- L Length, [m]
- p Pressure, [MPa]
- Pr Prandtl number
- Re Reynolds number
- T Temperature [K]
- ΔT_s Surface subcooling temperature [K]
- W mass fraction
- X Molar Fraction
- x vapor Quality
- X_{tt} Lockhart-Martinelli $X_{tt} = (1 - x/x)^{0.9}(\rho_v / \rho_l)^{0.5}(\mu_l / \mu_\rho)^{0.1}$ in eq. (4)

Greek symbols

- Δi_{lv} Latent heat, [Jkg^{-1}]
- ε^* Modified void factor
- λ Thermal conductivity, [Wm^{-1}K^{-1}]
- φ Lockhart-Martinelli two-phase parameter in eq. (4)
- ρ Density, [kgm^{-3}]
- θ liquid level angle subtended from the top of the tube (in radian) in eq. (4)

Subscripts

- a air
- b bulk
- c coil
- crit critical
- i inner
- l liquid
- LO liquid phase with total flow
- s steam
- sat saturation condition
- STRAT fully stratified flow regime
- v vapor
- w wall

Acronyms

AP1000	Advanced Passive 1000
APR1400	Advanced Power Reactor 1400
APR+	Advanced Power Reactor Plus
BWR	Boiling Water Reactor
CAREM	Central Argentina de Elementos Modulares
CS	Containment System
CLASSIC	Condensation Loop for Advanced Safety System in Containment
COSMEA	COndenSation test rig for flow Morphology and hEAt transfer studies
CUPID	Component Unstructured Program for Interfacial Dynamics code
DBA	Design Basis Accident
HTC	Heat Transfer Coefficient
HMTA	Heat and Mass Transfer Analogy
HX	Heat Exchanger
IRIS	International Reactor Innovative and Secure
ICS	Isolation Condenser System
iPOWER	Innovative Passive Optimised Worldwide Economical Reactor
KNGR	Korea Next Generation Reactor
LWR	Light Water Reactor
LOCA	Loss of Coolant Accident
MARS	Multi-Dimensional Analysis of Reactor Safety code
MSLB	Main Steam Line Break
NC	non-condensable
NPP	Nuclear Power Plant
PAFS	Passive Auxiliary Feedwater System
PASCAL	PAFS Condensing Heat Removal Assessment Loop
PCCS	Passive Containment Cooling System
POSTECH	Pohang University of Science and Technology
PRHRS	Passive Residual Heat Removal System
PSVCM	Pure Steam Vertical In-Tube Condensation Model
RELAP	Reactor Excursion and Leak Analysis Program

SG	Steam generator
SBO	Station Blackout
SBWR	Simplified Boiling Water Reactor
SMR	Small Modular Reactor
SMART	System-integrated Modular Advanced ReacTor
UCB	University of California at Berkeley

AUTHORS' CONTRIBUTIONS

The manuscript is written by Susyadi. Review and discussion by Susyadi, M. Juarsa, N. Putra, and R. A. Koestoer. All authors participated in the preparation of the final version of the manuscript.

REFERENCES

[1] Nayak, A. K., Sinha, R. K., Role of Passive Systems in Advanced Reactors, *Prog. Nucl. Energy, 49* (2007), 6, pp. 486-498
[2] Kim, W., *et al*., Extended Station Blackout Analyses of an APR1400 with MARS-KS, *Nucl Technol Radiat, 31* (2016), 4, pp. 318-326
[3] ***, Design Safety Considerations for Water Cooled Small Modular Reactors Incorporating Lessons Learned from the Fukushima Daiichi Accident, IAEA. Vienna, 2016
[4] Zeliang, C., *et al*., Integral PWR-Type Small Modular Reactor Developmental Status, Design Characteristics and Passive Features: A Review, *Energies, 13* (2020), 11, 2898
[5] Xing, J., *et al*., HPR1000: Advanced Pressurized Water Reactor with Active and Passive Safety, *Engineering, 2* (2016), 1, pp. 79-87
[6] Kang, K. H., *et al*., Separate and Integral Effect Tests for Validation of Cooling and Operational Performance of the APR+ Passive Auxiliary Feedwater System, *Nucl Eng Technol, 44* (2012), 6, pp. 597-610
[7] Schulz, T. L., Westinghouse AP1000 Advanced Passive Plant, *Nucl Eng Des., 236* (2006), 14-16, pp. 1547-1557
[8] Bae, B.-U., *et al.*, Experimental Investigation On Condensation Heat Transfer for Bundle Tube Heat Exchanger of the PCCS (Passive Containment Cooling System), *Ann. Nucl. Energy, 139* (2020), 107285
[9] Chen, R., *et al*., Steam Condensation on a Downward-Facing Plate in Presence of Air, *Ann. Nucl. Energy, 132* (2019), pp. 451-460
[10] de la Rosa, J. C., *et al*., Review on Condensation on the Containment Structures, *Prog. Nucl. Energy, 51* (2009), 1, pp. 32-66
[11] Yadav, M. K., An Integrated Approach to Steam Condensation Studies Inside Reactor Containments: A Review, *Nucl. Eng. Des., 300* (2016), pp. 181-209
[12] Huang, J., *et al*., Review of Vapor Condensation Heat and Mass Transfer in the Presence of Non-Condensable Gas, *Appl. Therm. Eng., 89* (2015), pp. 469-484
[13] ***, Safety Classification of Structures, Systems and Components in Nuclear Power Plants, Safety Standards for Protecting People and the Environment, Specific Safety Guide No. SSG-30. IAEA, Vienna, 2014
[14] ***, Passive Safety Systems and Natural Circulation in Water Cooled Nuclear Power Plants, IAEA, Vienna, 2009
[15] Kusuma, M. H., *et al*., Passive Cooling System in a Nuclear Spent Fuel Pool Using a Vertical Straight Wickless-Heat Pipe, *Int. J. Therm. Sci., 126* (2018), pp. 162-171
[16] Na, M. W., *et al*., Indefinite Sustainability of Passive Residual Heat Removal System of Small Modular Reactor Using Dry air Cooling Tower, *Nucl. Eng. Technol., 52* (2020), 5, pp. 964-974
[17] Mazzi, R., CAREM: An Innovative-Integrated PWR, *Proceedings*, 18th International Conference on Structural Mechanics in Reactor Technology (SMiRT 18), Beijing: International Association for Structural Mechanics in Reactor, 2005
[18] Sun, D. C., *et al*., Experimental Evaluation of Safety Performance of Emergency Passive Residual Heat Removal System in HPR1000, *Nucl. Eng. Des., 318* (2017), pp. 54-60
[19] Burgazzi, L., Failure Mode and Effect Analysis Application for the Safety and Reliability Analysis of a Thermal-Hydraulic Passive System, N*ucl. Technol., 156* (2006), 2, pp. 150-158
[20] Cho, Y. J., *et al*., Assessment of Condensation Heat Transfer Model to Evaluate Performance of the Passive Auxiliary Feedwater System, *Nucl. Eng. Technol., 45* (2013), 6, pp. 759-766
[21] Zhang, Y. P., *et al*., Design and Transient Analyses of Emergency Passive Residual Heat Removal System of CPR1000, *Nucl. Eng. Des., 242* (2012), pp. 247-256
[22] Schaffrath, A., *et al*., Operation Conditions of the Emergency Condenser of the SWR1000, *Nucl. Eng. Des., 188* (1999), 3, pp. 303-318
[23] Koo Kim, K., *et al*., SMART: The First Licensed Advanced Integral Reactor
[24] Carelli, M. D., *et al*., The Design and Safety Features of the IRIS Reactor, *Nucl. Eng. Des., 230* (2004), 1-3, pp. 151-167
[25] Lorenzo, G., *et al*., Reliability Assessment of the Thermal Hydraulic Phenomena Related to a CAREM-Like Passive RHR System, in Safety, Reliability and Risk Analysis: Theory, Methods and Applications, *Proceedings*, Joint ESREL and SRA-Europe Conference, 2009, pp. 2899-2907
[26] Reyes, J. N., NuScale Plant Safety in Response to Extreme Events, *Nuclear Technology, 178* (2012), 2, pp. 153-163
[27] Cuevas-Vasquez, D., *et al*., A Computational Methodology for Estimation of Aerosol Retention in a Sand-Bed Based Filtering System for Severe Accident Venting Strategies, *Nucl Technol Radiat, 35* (2020), 2, pp. 87-94
[28] Ha, H., *et al*., Optimal Design of Passive Containment Cooling System for Innovative PWR, *Nucl. Eng. Technol., 49* (2017), 5, pp. 941-952
[29] Kawakubo, M., *et al.*, An Experimental Study on the Cooling Characteristics of Passive Containment Cooling Systems, J. *Nucl. Sci. Technol., 46* (2009), 4, pp. 339-345
[30] Zhou, W., *et al*., Assessment of RELAP5/MOD3.3 Condensation Models for the Tube Bundle Condensation in the PCCS of ESBWR, *Nucl. Eng. Des., 264* (2013), pp. 111-118
[31] Jeon, B. G., No, H. C., Conceptual Design of Passive Containment Cooling System with Air Holdup Tanks in the Concrete Containment of Improved APR+, *Nucl. Eng. Des., 267* (2014), pp. 180-188
[32] Kral, P., *et al*., Sources and Effect of Non-Condensable Gases in Reactor Coolant System of LWR, in International Topical Meeting on Nuclear Reactor Thermal Hydraulics 2015, *Proceedings*, NURETH 2015, 2015, pp. 5194-5208

[33] Liu, L., *et al*., Effect of Surface Micromorphology and Hydrophobicity on Condensation Efficiency of Droplets Using the Lattice Boltzmann Method, *Therm. Sci., 26* (2022), 4B, pp. 3505-3515
[34] Baker, O., Design of Pipelines for the Simultaneous Flow of Oil and Gas, in Fall Meeting of the Petroleum Branch of AIME, Society of Petroleum Engineers, Apr. 1953
[35] Zhuang, X., *et al*., Two-Phase Flow Pattern Map for R170 in a Horizontal Smooth Tube, *Int. J. Heat Mass Transf., 102* (2016), pp. 1141-1149
[36] Shabestary, A. M., *et al*., Modelling of Passive Heat Removal Systems: A Review with Reference to the Framatome KERENA BWR Reactor: Part i, *Energies, 13* (2019), 1, 35
[37] 1929- Chato, John C., Laminar condensation inside horizontal and inclined tubes, Massachusetts Institute of Technology, USA, 1960.
[38] Boyko, L. D., Kruzhilin, G. N., Heat Transfer and Hydraulic Resistance During Condensation of Steam in a Horizontal Tube and in a Bundle of Tubes, *Int. J. Heat Mass Transf., 10* (1967), 3, pp. 361-373
[39] Chen, S. L., *et al*., General Film Condensation Correlations, *Exp. Heat Transf., 1* (1987), 2, pp. 93-107
[40] Dobson, M. K., Chato, J. C., Condensation in Smooth Horizontal Tubes, *J. Heat Transfer, 120* (1998), 1, pp. 193-213
[41] Sarma, P. K., *et al*., Convective Condensation Heat Transfer in a Horizontal Condenser Tube, *Int. J. Therm. Sci., 41* (2002), 3, pp. 295-301
[42] Cavallini, A., *et al*., Condensation of Halogenated Refrigerants Inside Smooth Tubes, *HVAC&R Res., 8* (2002), 4, pp. 429-451
[43] Cavallini, A., *et al*., Condensation in Horizontal Smooth Tubes: A New Heat Transfer Model for Heat Exchanger Design, *in Heat Transfer Engineering*, Taylor & Francis Group, New York, USA, 2006, pp. 31-38
[44] Geißler, T., *et al*., Experimental and Numerical Investigation of Flow Structure and Heat Transfer During High Pressure Condensation in a Declined Pipe at COSMEA Facility, *Int. Top. Meet. Nucl. React. Therm. Hydraul. 2015, NURETH 2015, 10* (2015), pp. 8547-8560
[45] Shah, M. M., An Improved and Extended General Correlation for Heat Transfer During Condensation in Plain Tubes, *HVAC&R Res., 15* (2009), 5, pp. 889-913
[46] Nie, Z., *et al*., Experimental Study on Condensation of High-Pressure Steam in a Horizontal Tube with Pool Boiling Outside, *Int. J. Heat Mass Transf., 108* (2017), pp. 2523-2533
[47] Akers, W. W., *et al*., Condensing Heat Transfer Within Horizontal Tubes, Chem. Eng. Progr., 1959
[48] Shah, M. M., A General Correlation for Heat Transfer During Film Condensation Inside Pipes, *Int. J. Heat Mass Transf., 22* (1979), 4, pp. 547-556
[49] Yun, B. Y., *et al*., Modeling of High Pressure Steam Condensation in Inclined Horizontal Tubes of PAFS in APR+, *J. Nucl. Sci. Technol., 53* (2016), 9, pp. 1353-1365
[50] Xu, H., *et al*., Experimental Study on the Effect of Wall-Subcooling on Condensation Heat Transfer in the Presence of Noncondensable Gases in a Horizontal Tube, *Ann. Nucl. Energy, 90* (2016), pp. 9-21
[51] Liu, H., *et al*., Experimental Investigation of a Passive Cooling Unit for Nuclear Plant Containment, *Nucl. Eng. Des., 199* (2000), 3, pp. 243-255
[52] Thome, J. R., *et al*., Condensation in Horizontal Tubes, Part 2: New Heat Transfer Model Based on Flow Regimes, *Int. J. Heat Mass Transf., 46* (2003), 18, pp. 3365-3387
[53] Amidu, M. A., *et al*., Performance Analyses of a Steam Condensation Tube Immersed in a Saturated Water Pool: Effects of Tube Inclination, *Nucl. Eng. Des., 323* (2017), pp. 142-155
[54] Abadi, S. M. A. N. R., Meyer, J. P., Numerical Investigation Into the Inclination Effect on Conjugate Pool Boiling and the Condensation of Steam in a Passive Heat Removal System, *Int. J. Heat Mass Transf., 12*2 (2018), pp. 1366-1382
[55] Rao, Y., *et al*., A Choice of Pure Steam Vertical In-Tube Condensation Model for Simulating A Passive Residual Heat Removal System, *Nucl. Eng. Des., 293* (2015), pp. 112-118
[56] Vierow, K. M., Schrock, V. E., Condensation in a Natural Circulation Loop with Noncondensable Gases, Part 1, 24. Japan Society of Multiphase Flow, Japan, 1991
[57] Oh, S., Experimental and Analytical Study of the Effects of Noncondensable Gas in a Passive Condenser System, Purdue University, USA, 2004
[58] Lee, K. Y., Kim, M. H., Experimental and Empirical Study of Steam Condensation Heat Transfer with a Noncondensable Gas in a Small-Diameter Vertical Tube, *Nucl. Eng. Des., 238* (2008), 1, pp. 207-216
[59] Kim, S. J., No, H. C., Turbulent Film Condensation of High Pressure Steam in a Vertical Tube, *Int. J. Heat Mass Transf., 43* (2000), 21, pp. 4031-4042
[60] Chung, Y.-J., *et al*., Wide Pressure Range Condensation Modeling on Pure Steam/Steam-Air Mixture Inside Vertical Tube, *Ann. Nucl. Energy, 118* (2018), pp. 140-146
[61] Lee, K.-Y., Kim. M. H., Effect of an Interfacial Shear Stress on Steam Condensation in the Presence of a Noncondensable Gas in a Vertical Tube, *Int. J. Heat Mass Transf., 51* (2008), 21-22, pp. 5333-5343
[62] Lee, K.-Y., Kim, M. H., Experimental and Empirical Study of Steam Condensation Heat Transfer with a Noncondensable Gas in a Small-Diameter Vertical Tube, *Nucl. Eng. Des., 238* (2008), 1, pp. 207-216
[63] ***, Design of Reactor Containment Systems for Nuclear Power Plants, IAEA, Vienna, 2004
[64] Lee, Y. G., *et al*., An Experimental Study of Air-Steam Condensation on the Exterior Surface of a Vertical Tube Under Natural Convection Conditions, Int. J. Heat Mass Transf., 2017
[65] Dehbi, A. A., The Effect of Noncondensable Gases on Steam Condensation Under Turbulent Natural Convection Conditions, Massachusetts Institute of Technology, USA, 1991
[66] Fan, G., *et al*., Development of a New Empirical Correlation for Steam Condensation Rates in the Presence of Air Outside Vertical Smooth Tube, *Ann. Nucl. Energy, 113* (2018), pp. 139-146
[67] Uchida, H., *et al*., *Evaluation of Post-Incident Cooling Systems of Light Water Power Reactors*, Tokyo University, Japan, 1964
[68] Su, J., *et al*., Experimental Study of the Effect of Non-Condensable Gases on Steam Condensation Over a Vertical Tube External Surface, *Nucl. Eng. Des., 262* (2013), pp. 201-208
[69] Anderson, M. H., *Steam Condensation on Cold Walls of Advanced PWR Containments*, The University of Wisconsin – Madison, Ann Arbor, 1998
[70] Kim, J. W., *et al*., Condensation Heat Transfer Characteristic in the Presence of Noncondensable Gas on Natural Convection at High Pressure, *Nucl. Eng. Des., 239* (2009), 4, pp. 688-698

[71] Dehbi, A., A Generalized Correlation for Steam Condensation Rates in the Presence of Air Under Turbulent Free Convection, *Int. J. Heat Mass Transf., 86* (2015), pp. 1-15

[72] Tagami, T., Interim Report on Safety Assessments and Facilities Establishment Project for June 1965. Japanese Atomic Energy Research Agency, Japan, 1965

[73] Skolik, K., *et al.*, LOCA-Type Scenario Simulation for NuScale-SMR with RELAP/SCDAPSIM/MOD3.4, Proceedings, 18th Int. Top. Meet. Nucl. React. Therm. Hydraul. NURETH 2019, 2019, pp. 6690-6700

[74] Skolik, K., *et al*., Analysis of Loss of Coolant Accident Without ECCS and DHRS in an Integral Pressurized Water Reactor Using RELAP/SCDAPSIM, *Prog. Nucl. Energy, 134* (2021), p. 103648

[75] Susyadi, M., *et al*., An Alternative Cooling Solution During Loss of Coolant Accident with Emergency Core Cooling System Failure in NUSCALE Nuclear Reactor, *Prog. Nucl. Energy, 169* (2024), p. 105063

Received on September 1, 2023
Accepted on February 28, 2024

СУСЈАДИ, Мулја ЏУАРСА, Нанду ПУТРА, Ралди А. КЕСТЕР

ПРОУЧАВАЊА ПОВРШИНСКЕ КОНДЕНЗАЦИЈЕ СИСТЕМА ПАСИВНЕ СИГУРНОСТИ У ЛАКОВОДНОМ РЕАКТОРУ – ПРЕГЛЕД

Сматра се да систем са пасивним механизмом има бољу поузданост јер не захтева спољну покретачку снагу да би функционисао. Неколико дизајна нуклеарних реактора имплементирало је ову карактеристику у својим сигурносним системима, било у потпуности или делимично. Неки од њих комбинују појаве кључања и кондензације како би се изборили са заосталом топлотом када се догоди акцидент. У овом раду приказане су истраживања о преносу топлоте кондензације у пасивним системима за уклањање преостале топлоте и пасивним системима контејмента за хлађење реактора лаком водом. Акценат је на примењивости прихваћених корелација за услове удеса и њиховом развоју за бољи модел. У образложењу, најпре се идентификују пасивни механизам и тип кондензатора који је имплементиран у систем. Затим се расправља о компаративној процени формуле коришћењем тест података, параметарским студијама коришћењем компјутерске симулације и развоју нових корелација. Евалуација је показала да коришћење постојеће корелације захтева подешавање у случају пројектовања пасивног сигурносног система лаководног реактора. Поред тога, предложено је да се узме у обзир геометријски облик кондензационе површине. Потребна су даља истраживања спиралног облика да би се проценила могућност промене улоге генератора паре интегралног реактора као кондензатора током удеса губитка расхладне течности, који је праћен пропустом безбедносног система.

Кључне речи: кондензација, сигурносни систем, одвођење топлоте, лаководни реактор, акцидент